J Mater Sci (2011) 46:2397–2409
DOI 10.1007/s10853-011-5264-7

REVIEW

One-dimensional 8-hydroxyquinoline metal complex nanomaterials: synthesis, optoelectronic properties, and applications

Zhigang Yin · Bingxi Wang · Guihua Chen · Mingjian Zhan

Received: 25 September 2010 / Accepted: 6 January 2011 / Published online: 19 January 2011

Abstract One-dimensional (1D) 8-hydroxyquinoline metal complex nanomaterials exhibit distinctive characteristics that differ from those of their bulk counterparts. Owing to their small size, shape anisotropy, unique structures, and novel properties, these organometallic 1D nanostructures are promising candidates for various devices. This review highlights current progress in the synthesis of 1D 8-hydroxyquinoline metal complex nanomaterials and summarizes their optoelectronic properties and applications. The mainly synthetic strategies are divided into three categories, which include vapor phase growth, solution phase growth, and self-assembly. Special attention is paid to the formation mechanisms and the control measures for 1D nanostructured 8-hydroxyquinoline metal complexes. Other new methods such as template-based synthesis and electrospinning are briefly described. Merits and shortcomings of each synthetic strategy are simply discussed. Then, a variety of optoelectronic properties including luminescence, field emission, charge transport, photoconductivity, and photo-switching properties are reviewed, and their applications in optoelectronic devices, field emission, and templates are also surveyed. In the end, concise conclusions are provided, and personal perspectives on future investigations of 1D 8-hydroxyquinoline metal complex nanomaterials are proposed.

Z. Yin · B. Wang (✉) · G. Chen · M. Zhan
College of Materials Science and Engineering, Fuzhou University, Fuzhou 350108, Fujian, People's Republic of China
e-mail: wangbx@fzu.edu.cn

Z. Yin
e-mail: zhigangy@hotmail.com

Introduction

Since the strong electroluminescence (EL) of low-voltage organic light-emitting diodes (OLEDs) based on tris(8-hydroxyquinoline) aluminum (AlQ_3) first discovered by Tang and VanSlyke [1] in 1987, 8-hydroxyqunioline metal complexes (MQ_n, M = metal, HQ = 8-hydroxyquinoline, Q = deprotonated 8-hydroxyquinoline, n = ligand number), have attracted considerable attention because of their wide applications in OLED devices as excellent electron-transporting and emitting materials. Among the MQ_n family, AlQ_3 is most well known and frequently used due to its high stability, good charge transport ability, and strong luminescence emission [2–4]. Compared to AlQ_3, GaQ_3 could provide an approximately 50% higher power efficiency in light-emitting devices [5], while ZnQ_2 showed a characteristic of lower opening voltage [6]. CdQ_2 also displayed luminescent property and was expected to be applied in optoelectronic devices [7, 8]. In addition, other MQ_n complexes or HQ derivative metal complexes such as BeQ_2, MgQ_2, $ZnMQ_2$, and $BeMQ_2$ (where M = methyl) as well as $AlPrQ_3$ (where Pr = propyl) were served as efficiently emitting and electron-transporting materials for the fabrication of OLED devices, all of which had a luminance of more than 3000 cd/m^2 [9].

In order to improve the efficiency and performance of these MQ_n complexes, their hybrid materials were proposed by Khaorapapong et al. and other groups [10–16]. By incorporating various metal complexes including LiQ, ZnQ_2, MnQ_2, and AlQ_3 into the interlayer of smectites via solid–solid reactions, the resultant hybrid materials could display enhanced luminescence as compared with the corresponding pure complexes owing to the host–guest interactions [10–13].

On the other hand, size reduction of MQ_n complexes into nanostructures may lead to novel characteristics,

improved performances and new applications [17–25], resulting from the size effect [26–28], surface effect [29, 30], macroscopic quantum tunneling effect [31, 32], and others [33–35]. Especially, one-dimensional (1D) MQ_n complexes, such as nanorods, nanowires, nanobelts, and nano-arrays, have gained much attention during past 8 years. There were several unique optoelectronic properties of them reported including luminescence, field emission, charge transport, photoconductivity, and photo-switching, which encouraged intensive application researches related to OLED devices, sensors, field emission, low-threshold mirrorless lasing, and circularly polarized emission, as well as promising materials for waveguide [36–44]. It can be seen that 1D MQ_n complex nanomaterials provide a good system to investigate the functional organometallic complexes and their nanostructures. Consequently, it is expected that these anisotropic MQ_n complex nanomaterials could open a new area in optoelectronics and serve as test beds to address general fundamental optoelectronic issues.

This review focuses on recent developments of the synthetic strategies, optoelectronic properties, and applications of 1D nanostructured MQ_n complexes and their derivatives. In first section, a brief description for the background of MQ_n complexes is presented. In second section, the synthetic strategies for various 1D MQ_n complex nanomaterials are systematically highlighted. In third and fourth sections, the unique optoelectronic properties and applications of 1D nanostructured MQ_n complexes are summarized, respectively. At the end of this review, simple conclusions and outlook on these 1D nanoscale complexes are proposed.

Synthetic strategies for achieving 1D MQ_n complex nanomaterials

In this section, we present a comprehensive overview of synthetic strategies for 1D MQ_n complex nanomaterials. The strategies are broadly categorized into three groups: (1) vapor phase growth, (2) solution phase growth, and (3) self-assembly. Other methods such as template-based synthesis and electrospinning have also been briefly reviewed. The possible formation mechanisms and control measures of these organometallic 1D nanostructures are specially discussed.

Vapor phase growth

Vapor phase growth is one of most effective strategies for the synthesis of 1D MQ_n complex nanomaterials. In this method, various 1D nanostructures are prepared by simple evaporation and deposition processes under an appropriate gas atmosphere, the structure and size of which can be controlled by regulating working temperature, working pressure, working gas, and gas flow rate. The formation of 1D nanostructures mainly depends on the control of nucleation and growth in the crystallization. So far, there have been many approaches to synthesize MQ_n complex nanorods, nanowires, nanobelts, and ordered 1D nanoarrays, such as vapor condensation [45–49], simple physical vapor deposition (PVD) [50–52], glancing angle deposition (GLAD) [53, 54], and other vapor phase techniques [55, 56], which have achieved a series of significant successes.

Among them, the most remarkable work was pioneered by Wang and Perng's group in 2003 [45, 46]. They were the first to use vapor condensation system (Fig. 1a) with liquid nitrogen as the cooling source and indium tin oxide (ITO)-coated glass electrode as the growth substrate, successfully synthesized amorphous AlQ_3 nanowires with 30–50 nm in diameter and AlQ_3 nanobelts with 40–60 nm in width (Fig. 1b). In the schematic formation diagram of these 1D AlQ_3 nanostructures as shown in Fig. 1c, the corresponding growth mechanism was different from the vapor–liquid–solid (VLS) model [57]. It was proposed that the evaporated AlQ_3 molecules collided with Ar atoms and were then rapidly cooled to form nanobelts. The released heat of sublimation might induce a narrow temperature inversion region in the vapor–solid (VS) interface to build the trunks of nanowires. This growth mechanism was similarly employed in the trunk surface, thus secondary and tertiary branches were further formed, finally resulting in numerous dendritic AlQ_3 nanowires. Such a vapor growth method has opened an available way to synthesize 1D MQ_n complex nanomaterials. The potential application will be of great interest to future study. On this basis, the GaQ_3 nanowires were likewise prepared by this method [49]. And it has been realized that a lower working pressure and a lower working temperature would contribute to produce smaller diameter of AlQ_3 and GaQ_3 nanowires; on the contrary, larger nanoparticles were formed [48, 58].

As above mentioned, the vapor condensation method is greatly influenced by different working parameters, which provide a lot of effective measures for the control synthesis of 1D MQ_n complex nanomaterials. However, it should be noted that this method needs some harsh conditions such as high temperature and liquid nitrogen cooling, and also it has some difficulties in preparing ordered 1D nanoarrays and well-crystallized products. These defects will prevent its further utilization. Therefore, it remains a desirable target to develop convenient, mild, and practical vapor phase growth techniques and to optimize the synthetic process, which has gradually become the focus of attention. According to the vapor condensation method combined with a one-step heat treatment, for the first time, Perng's group [55, 56] found that amorphous AlQ_3 nanoparticles or thin film directly grew into α-phase crystalline AlQ_3

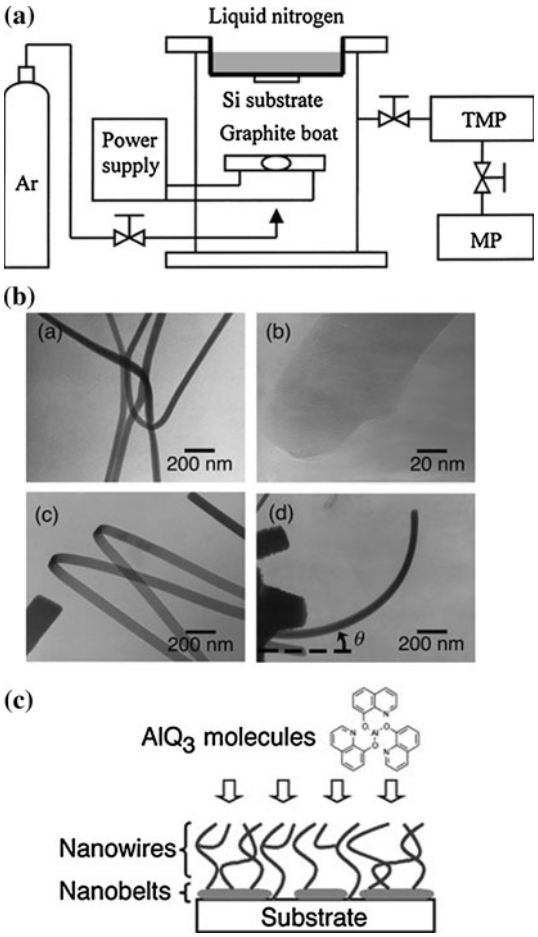

Fig. 1 **a** Experimental setup of the vapor condensation system. **b** Transmission electron microscopy (TEM) images of the 1D AlQ_3 nanostructures: (*a*) TEM image of the AlQ_3 nanowires; (*b*) high-resolution TEM (HRTEM) image of a typical AlQ_3 nanowire (no lattice image is observed, which refers to an amorphous structure); (*c*) TEM image of the AlQ_3 nanobelts, and (*d*) an AlQ_3 nanobelt rolled up along the axial direction after irradiated by the electron beam in TEM. **c** Schematic formation diagram of the 1D AlQ_3 nanostructures [45, 46]

nanowires under appropriate Ar pressure, heating temperature, and heating time. The growth of these nanowires was controlled by the anisotropic crystallographic nature of α-AlQ_3 [59]. The formation mechanism could be illustrated by the concept of nucleation and molecular migration within the film or nanoparticles. Using an adsorbent-assisted physical vapor deposition (AA-PVD) method, single-crystalline AlQ_3 nanowires were successfully prepared from functional AlQ_3 molecules by Zhao et al. [50]. The introduction of the adsorbents such as neutral aluminum oxide or silica decreased the sublimation temperature and slowed down the weight loss of AlQ_3, through which the degree of saturation and the uniformity of the nanowires could be controlled. No catalyst was used and no droplet was found at the top, so the growth of the AlQ_3 nanowires prepared with this method should be abided by the VS process [60].

Recently, GLAD method has also been proven to be an efficient and versatile technique to construct AlQ_3 thin film composed of ordered 1D AlQ_3 nanoarrays with controllable morphologies and dimensions. Figure 2 shows the typical helical AlQ_3 nanorod arrays which were prepared with different deposition angles and turn numbers [37]. Despite that the exact growth mechanism of these uniform porous AlQ_3 nanorod arrays remains under investigation, we think it may be similar to the formation of highly ordered AlQ_3 chiral luminescent thin films via the GLAD process reported by Brett et al. [53]. Obviously, GLAD method offers an advanced level of engineering control over MQ_n complex 1D nanoarrays, and some complicated, porous, film-based photonic heterostructures. This vapor phase method is believed to largely facilitate the fabrication and application of devices in the fields of optics, electronics, and sensors.

In a word, the above vapor phase routes to 1D MQ_n complex nanomaterials have the dominant advantages of both "access to highly regular 1D nanostructure" and "controlled synthesis." But the harsh experimental conditions and low productivity will hinder their follow-up applications to some extent.

Solution phase growth

Solution phase growth technique has drawn considerable attention because of its virtues such as simple synthesis procedure, easy operation, and high efficiency in comparison with the vapor phase growth. For this approach, solution–liquid–solid (SLS) mechanism [61, 62] is expected to be the main growth mechanism for the synthesis of abundant 1D nanostructures. How to choose appropriate solution reaction conditions and control the degree of supersaturation, nucleation as well as anisotropic growth process, to some extent, is the key to this strategy used to prepare 1D MQ_n complex nanomaterials.

Based on the solution phase growth, various 1D MQ_n complex nanomaterials can be synthesized by a facile hydrothermal or solvothermal route. Reaction temperature, reaction time, pressure, reactant concentration, surfactant type and concentration, solvent medium, and pH value are the main influential factors to the size and morphology of products. For instance, the amorphous AlQ_3 nanorods were prepared from the hydrothermal reaction of HQ and aluminum nitrate at 120 °C for 12 h [63]. The sodium dodecyl benzene sulfonate (SDBS) played a crucial role in the formation of these nanorods; meanwhile, reaction time and temperature also influenced the quality of the final products. We suppose that this new kind of surfactant-assisted

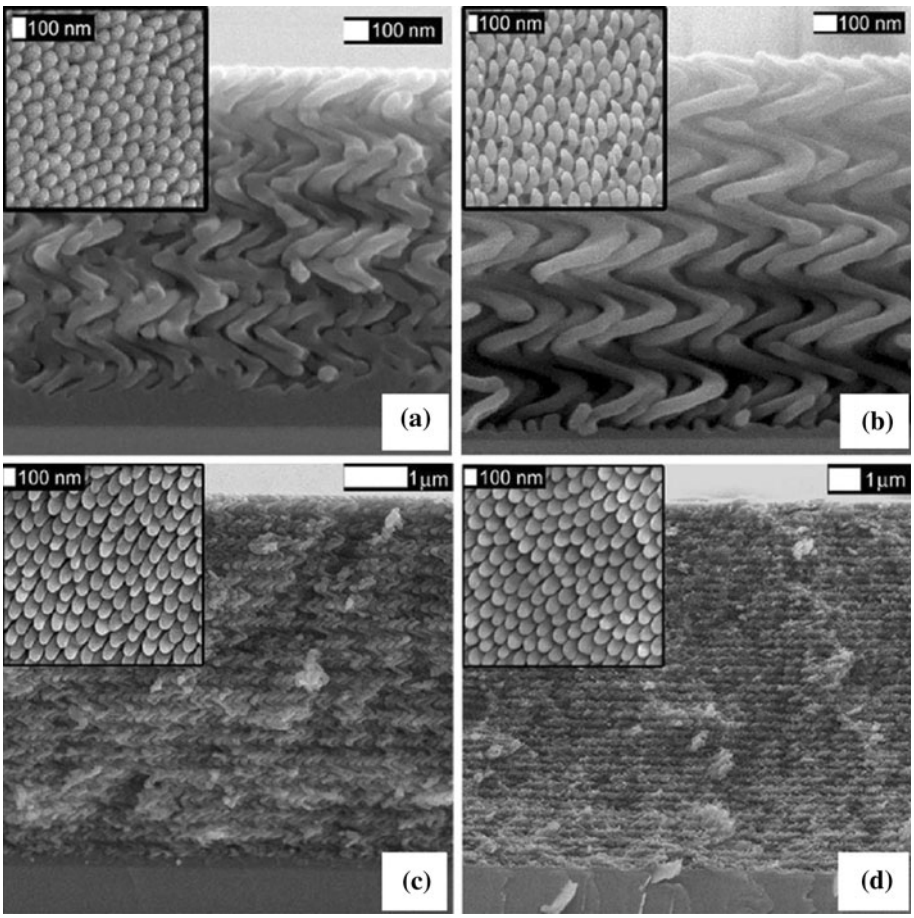

Fig. 2 Scanning electron microscopy (SEM) images (section view) with *insets* of the plan views for helical AlQ_3 nanorod arrays deposited at different turn numbers and deposition angle: **a** A 5-turn sample deposited at 75°; **b** a 5-turn sample deposited at 85°; **c** a 19-turn sample deposited at 78°; and **d** a 40-turn sample deposited at 78° [37]

hydrothermal route can be extended to synthesize other organometallic 1D nanomaterials.

Likewise, a simple solvothermal process was proposed for the synthesis of luminescent CdQ_2 nanorods and nanoflowers (bundles of nanorods) in an oleic acid–sodium oleate–ethanol–hexane (or not)–H_2O system at 55–100 °C [7]. In this synthetic route, shown in Fig. 3, the sodium oleate (NaOA) was formed initially and then coordinated with Cd^{2+} to produce cadmium oleate, which released Cd^{2+} slowly based on the equilibrium equation to control the nucleation and growth process accurately. The NaOA could also joint with the superfluous oleic acid to generate a buffer media, which was lucrative for the precipitation between Cd^{2+} and HQ [64]. On the other hand, the interactions such as Van der Waals interaction and the hydrophobic force between the alkyl chain and quinoline ring would make it easier for HQ molecules to collide with Cd^{2+} capped on the surface of NaOA to start the main reaction. At last, the CdQ_2 products were precipitated due to their lower solubility. It was proposed that higher concentrations of the reactants and the surfactant with a lower temperature and a shorter reaction time would result in the formation of nanorods, whereas a longer time and a higher temperature led to nanoflowers. The obtained CdQ_2 nanorods with excellent photoluminescence (PL) properties can be considered as the building blocks for novel optoelectronic nanodevices.

Changing the solvothermal environment, other kinds of 1D MQ_n complex nanomaterials, such as AlQ_3 [42], ZnQ_2 [43], and CdQ_2 [65] nanoribbons, were also prepared without any assistance of surfactants and templates. The final structure and size of nanoribbons can be determined by reaction temperature, heating time, and pH value, despite the detail mechanism is not clear yet. This facile solvothermal methodology may be extended for the controlled large-scale synthesis of other functional 1D organometallic nanomaterials.

Chemical precipitation, which is another generally used solution phase growth method, has been proven to be a very simple and versatile way to prepare organic, inorganic, and orgaometallic 1D nanomaterials [25, 66–68]. The formation of precipitation always involves two processes: nucleation and growth, which can be efficiently controlled by different reaction conditions similar to the hydrothermal and solvothermal routes. With this method, for example, our group [69] have successfully synthesized abundant 1D

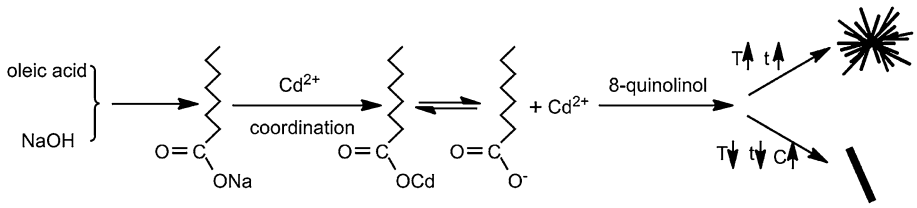

Fig. 3 Schematic diagram showing the formation of CdQ_2 nanorods and nanoflowers [7]

nanostructured copper(II) 8-hydroxyquinolinate (CuQ_2) with polymorphs by simply adjusting ethanol–water reaction medium (shown in Fig. 4). The XRD and SEM results showed that the poor crystallized α-CuQ_2 dihydrate nanorods were precipitated rapidly from the coordination reaction of reactants in aqueous solution. The nanorods were around 40–130 nm in diameter and 0.5–2 μm in length (Fig. 4b, c). Control of the reaction medium in ethanol–water solutions (total ethanol/water volume ratio of 3:1), the mixed α-, γ-, and β-phase crystallized CuQ_2 dihydrate nanostructures were produced quickly. In these mixed structures, the dominant nanowhisker had an average diameter of about 280 nm (Fig. 4d, e). As to the reaction medium of pure ethanol, however, the novel α-form anhydrous CuQ_2 micro-scale lath bundles were assembled from nanolaths whose thickness and width are about 300 and 800 nm, respectively (Fig. 4f, g). The formation of these 1D CuQ_2 nanomaterials was believed to be directed by the crystal habit and growing environment. Different ethanol–water media not only could affect the molecular structure and aggregation of CuQ_2, but also could provide discrepant surroundings for the crystal growth [70], which resulted in the products with various morphologies and polymorphs. This facile, rapid, and convenient approach offers an efficient solution phase route to synthesize other 1D nanomaterials with controllable morphologies and crystal phases.

In addition, sonochemical synthesis [71, 72] and one-step seed method [73] have also been served as facile solution-based growth techniques to prepare 1D MQ_n complex nanomaterials, including AlQ_3 nanobelts, CdQCl nanowires, and AlQ_3-ZnO hybrid nanofibers. The exact growth mechanisms of these methods are not yet ripe due to few literatures reported.

It can be seen that the advantages of solution phase growth are simple, efficient, low-cost, and easy to industrialization. But building 1D nanoarrays and composite 1D nanostructures are still a bottleneck for most of the existing solution phase methods. Also, the current study shows a monotonous state, and the universal synthetic method remains few and poor. Accordingly, we believe that the strategy of solution phase growth should be used to combine with template-based synthesis, self-assembly, and other useful methods so as to more effectively construct a variety of 1D nanostructures and their devices.

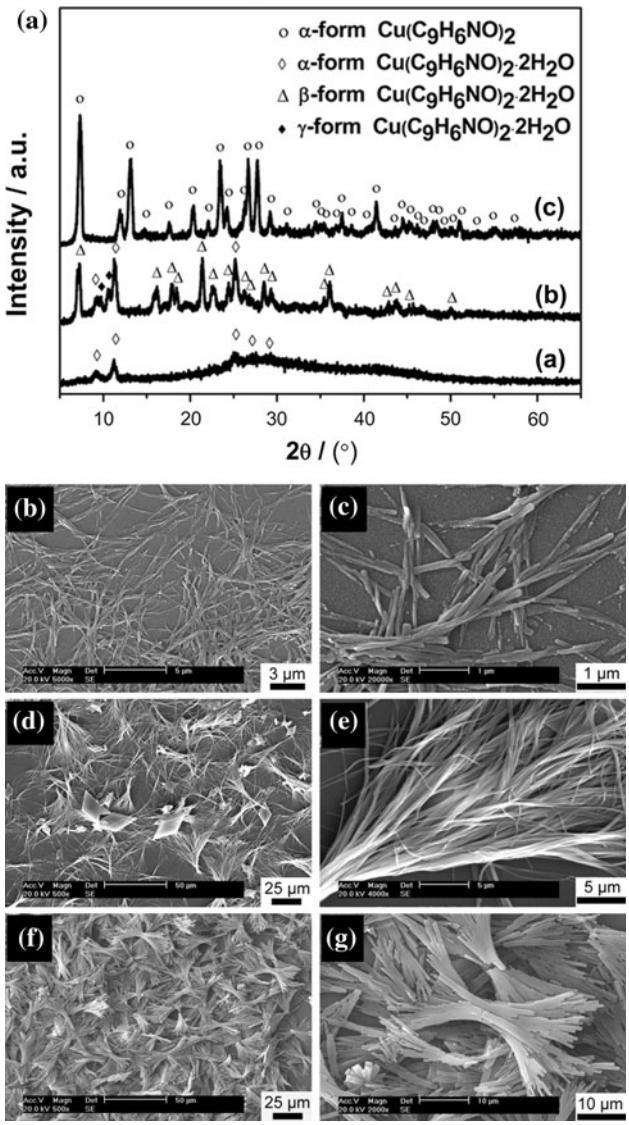

Fig. 4 XRD patterns of **a** CuQ_2 synthesized in different ethanol–water media: (*a*) aqueous solution; (*b*) ethanol aqueous solution (ethanol/water = 3:1); and (*c*) ethanol solution. SEM images of CuQ_2 synthesized in different ethanol–water media: **b–c** aqueous solution, **d–e** ethanol aqueous solution (ethanol/water = 3:1), and **f–g** ethanol solution [69]

Self-assembly

Self-assembly is widely used in the synthesis of 1D nanostructured MQ_n complexes and their derivatives.

Generally, it is accomplished by non-covalent interactions of building unites to form aggregates spontaneously. The assembly of molecules and nanoparticles to nanoscale 1D structures needs the driving forces from themselves and sometimes initiation from the surroundings [25].

At present, there are two main types of self-assembly for the synthesis of 1D MQ_n complex nanomaterials. The first one is based on the micellar growth of surfactant-assisted self-assembly [41, 44, 71]. In this way, surfactant plays dual roles in the formation of 1D nanostructures. The molecules of surfactant assemble into some micelles which can offer the necessary conditions for oriented growth of MQ_n complexes. On the other hand, the formed 1D nanomaterials can be stabilized and dispersed by the surfactant molecules. It should be noted that this method can be used to obtain highly uniform and monodisperse 1D nanostructures, whose sizes would be larger than that of the products synthesized by vapor or solution phase growth methods. For example, a facile self-assembly route assisted by cetyltrimethyl ammonium bromide (CTAB) was developed to synthesize α-AlQ_3 nanorods with regular hexagonal shape and a diameter of 400 ± 20 nm [41]. It was found that the AlQ_3 nanorods were single-crystalline structures with preferential growth along the [001] direction. Nevertheless, questions about the exact mechanism remained, and more intensive studies were required to understand this self-assembly process.

Using the similar approach, a facile emulsion-based route was designed by Chen et al. [74] for the large-scale synthesis of monodisperse AlQ_3 nanorods with regular hexagonal prism morphology (Fig. 5a, b). They focused on the self-assembly process and proposed a tentative growth mechanism (Fig. 5c) for the formation of AlQ_3 nanorods. At the beginning, a normal microemulsion of $CHCl_3$ in H_2O was formed by assistance of CTAB. When the emulsion was heated, the chloroform in micelles volatilized into the atmosphere causing the concentration of AlQ_3 in these micelles to increase and eventually supersaturated which led to nucleation. Once the chloroform in a micelle was depleted, the nuclei moved from the hydrophobic inner core of the micelle to the hydrophilic, cationic headgroups of CTAB bilayers produced in the water phase. These bilayers were formed in a "zipping" manner by superfluous CTAB molecules through Van der Waals and hydrophobic interactions [75]. The reason for the position transfer process of the nuclei was that the coulomb attraction between CTAB and AlQ_3 molecules was much stronger than the Van der Waals interaction between the alkyl chains of CTAB and the quinoline rings of AlQ_3. Finally, the bilayer micelles induced the anisotropic growth of nuclei to longer

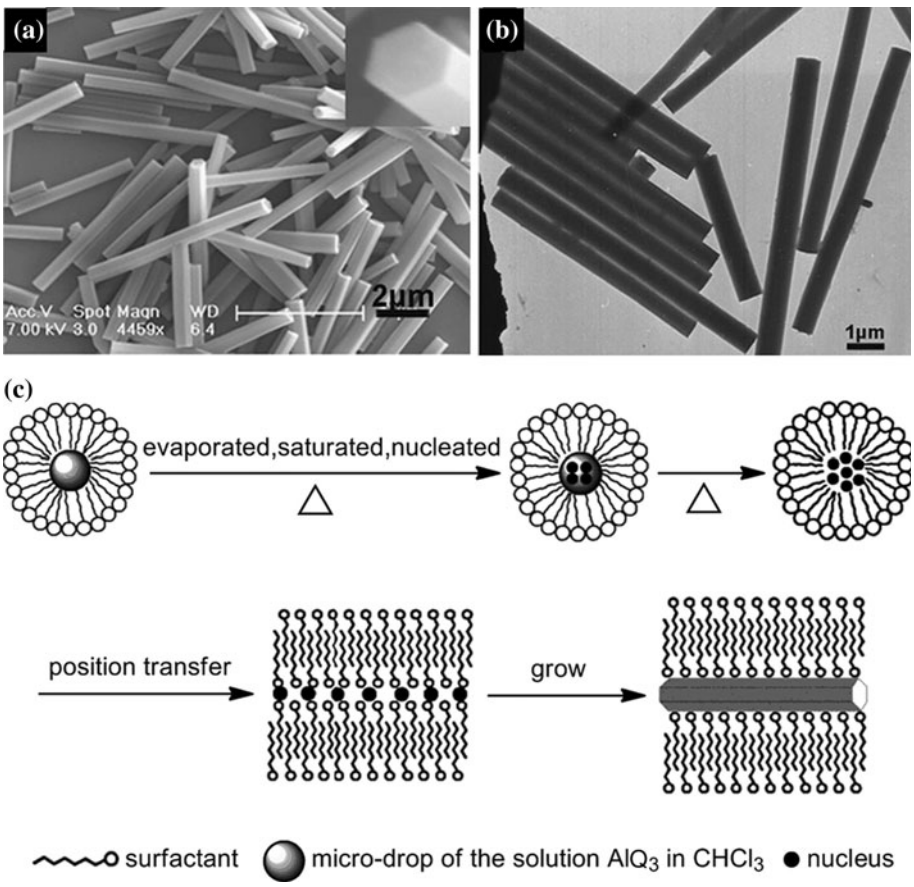

Fig. 5 **a** Field emission scanning electron microscopy (FESEM) image of AlQ_3 nanorods (*Inset*: cross-sectional view of one typical rod). **b** TEM image of AlQ_3 nanorods. **c** Schematic illustration of the proposed formation mechanism of AlQ_3 nanorods [74]

nanorods by acquiring raw material from other micelles. It demonstrated that the size and morphology of the AlQ_3 nanorods could be modified by both concentration and type of the surfactant. The depicted mechanism and control measures in this study could be extended to other systems for controlled synthesis of 1D nanomaterials.

The second one is the non-micellar self-assembly through non-covalent intermolecular interactions, such as solvent-evaporation-induced self-assembly [38], organogelation self-assembly [76–78], etc. In comparison with the self-assembly of micellar system, this approach does not need surfactant assistant, thus avoiding the residue of it on the surface of nanostructures may significantly weaken the performance of the materials. Organogelation self-assembly, one of the most representative examples, has been demonstrated as an efficient method for the synthesis of various 1D nanoscale gels [79]. The low-molecular weight gels, which have the crystal-like nature unlike the dynamic nature characteristic of micellar systems, are produced by non-covalent interactions including Van der Waals force, hydrogen bonding, and π–π stacking between gelator molecules and solvent molecules [25, 76].

The 3,4,5-tris(n-dodecyloxy)-benzoylamide substituents appended 8-qinolinol copper(II)-, palladium(II)-, and platinum(II)-chelates (1M, M = Cu, Pd, Pt) were reported as highly efficient gelators for various organic solvents to form the 1M gel nanofibers [76, 77]. As displayed in Fig. 6, the organogels were obtained by the gelation of *p-xylene* by 1M. The TEM images shown in Fig. 6a–c suggested that well-developed networks consisted of fibrous aggregates, and the approximate diameter and the length of the fibrous aggregate of the 1M + *p-xylene* gels were being 10–50 nm and several micrometers, respectively. The gel formation was attributed to the strong π–π interactions of chelate moieties and the hydrogen bond interactions among the amide groups. On the other hand, the introduction of the 3,4,5-tris(n-dodecyloxy)-benzoylamide substituents into a π-conjugated planar molecule was favorable for self-assembly into a columnar-stacking structure to give highly ordered gel nanofibers [80–84]. A packing structure shown in Fig. 6d(b) was proposed as the most probable aggregation model. The distance of the intercolumnar separation (42 Å) was shorter than the molecular length of 1M (ca. 52 Å). This result implied that the molecules in the gels were stacked in a tilted fashion along the *c*-axis (Fig. 6d(c)). As clearly observed in Fig. 6d(d), these π–π stacked structures along the *c*-axis were visually confirmed by HRTEM as strong stripe contrasts parallel to the axis along the length of the fiber. Recently, the 5-(cholesteryloxy)methyl-8-hydroxyquinoline lithium(I) (LiChQ) was

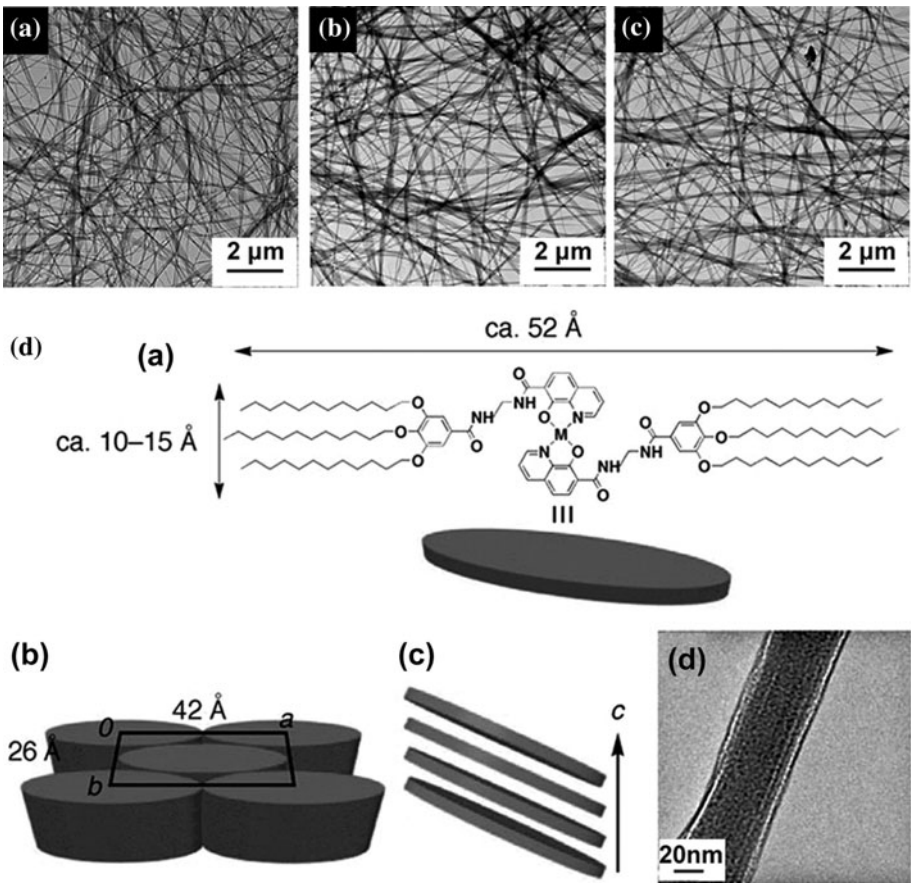

Fig. 6 **a–c** TEM images of the 1M + *p-xylene* gels: **a** 1Cu, **b** 1Pd, **c** 1Pt, [1M] = 1.0 mg mL^{-1}. **d** (*a*) molecular scales of 1M; (*b*) proposed packing model of 1M in the gel tissues; (*c*) tilted arrangement of 1M along the *c* axis; and (*d*) an HRTEM image of the 1Pt + *p-xylene* gel: [1Pt] = 2.0 mg mL^{-1} [77]

synthesized through the modification of LiQ with cholesterol, and then LiChQ gel nanofibers of 30–100 nm diameter were obtained in non-protic organic solvents through self-assembly in a super-gel state [78].

There is no doubt that the growth of self-assembly provides a strong impetus to promote the synthesis and application of 1D nanoscale MQ_n complexes and their derivatives with novel structures and unique properties, whereas it should be pointed out that the current routes to these 1D nanomaterials are still poor-controllable and slightly complicated. Therefore, how to overcome the shortcomings and highlight the strengths to make full use of self-assembly will be a great challenging topic in this field.

Other methods

Except for the main vapor phase growth, solution phase growth and self-assembly as described above, other strategies such as template-based synthesis [85, 86], electrospinning [87–89], low-temperature solid phase reaction [90], and double-film annealing [91] have all been employed to synthesize 1D MQ_n complex nanomaterials. But it should be noted that there are only few reports on them. Among, template-based synthesis requires nanostructured materials as "hard" or "soft" templates, such as zeolite, porous anodic aluminum oxide (AAO) membrane and polycarbonate (PC) film, carbon nanotube, liquid crystal, polymer, etc. [92–94], to promote in situ growth and control of 1D nanostructures depending on the shape and size of the templates. Recently, the polycrystalline ZnQ_2 nanorod arrays were fabricated by in situ liquid–liquid interfacial precipitation in the pores of AAO membranes [85]. It is pretty easy to obtain well-controlled size and morphology of 1D nanostructure by template method, however, the templates used need to be pre-prepared and post-removed, which would increase the cost and risk of large-scale manufacture. Besides, electrospinning as a physical method has also been successfully used to fabricate highly fluorescent AlQ_3/PPV, AlQ_3/PEO, and AlQ_3/PVP nanofibers [87–89]. Obviously, this method has a distinctive advantage in the preparation of 1D nanostructures with a macro-scale dimension along the axial direction, and it can ensure the continuity of 1D nanostructures [95–97]. Nevertheless, it is still difficult for this method to prepare pure 1D MQ_n complex nanomaterials because they have poor processability and should be assisted by organic polymers.

Although the studies used these methods for the synthesis of 1D MQ_n complex nanomaterials just begin, and many details of them are still unclear, we believe that these strategies have the great prospects to fabricate 1D nanostructures of functional complexes. In particular, the template method and the electrospinning technique would be the focus of future development in this area, and it is necessary and significant to carry out related research work.

Optoelectronic properties of 1D MQ_n complex nanomaterials

It is generally accepted that low-dimensional nanostructures exhibit distinct optical, electronic, chemical, and physical properties because of their large surface areas and possible quantum confinement effects. On this basis, many efforts have been made to investigate the novel optical and electronic properties of the 1D nanostructured MQ_n complexes which differ from their bulk materials. In this section, we briefly summarize the current studies on the optoelectronic properties of various 1D MQ_n complex nanomaterials.

Luminescence

PL and EL are the extremely important optoelectronic characteristics of organic light-emitting materials. Although the so-called quantum effect has not been observed so far, a series of unique PL and EL behaviors have been obtained in 1D nanostructured MQ_n complexes and their derivatives, which result from their structural transformation in nature.

To start with, it has been realized that molecular configuration, composition, size, and morphology of 1D MQ_n complex nanomaterials play the essential roles in determining their luminescent properties. For example, a study [50] revealed that the PL spectra of as-prepared AlQ_3 nanowires showed emission of an interesting fine structure on increasing the excitation energy, which was attributed to the ordered orientation of the AlQ_3 molecules in the nanowires. More importantly, these AlQ_3 nanowires could be fabricated into an EL device, which exhibited excellent optoelectronic properties with an obvious size-dependent effect. A similar size-dependent performance was reported by Li's group [7], which was ascribed to the larger surface area of the CdQ_2 nanorods with smaller size leading to enhanced absorption of UV light and stronger PL emission [17]. There was no obvious PL blue shift emerged in 1D MQ_n complex nanomaterials as their sizes shrank because the molecules were merely bonded together by weak Van der Waals forces [98]. In addition, highly ordering AlQ_3 chiral thin films composed of helical nanorod arrays were fabricated to explore novel optical properties. Interestingly, these unique 1D nanostructures of AlQ_3 selectively transmitted one handedness of circularly polarized light and also generated circularly polarized PL [53]. These findings will

be found uses in optoelectronics, chemical sensors, and photovoltaics.

Furthermore, it is found that the crystallinity and crystal phase are important influential factors to the luminescent properties of 1D MQ_n complex nanomaterials. Perng's group [55, 56] reported that an enhanced PL intensity and a spectral blue shift were observed on the AlQ_3 nanowires grown from amorphous AlQ_3 thin film or nanoparticles by a heat-treatment process (Fig. 7), which could be attributed to the predominantly formed α-phase AlQ_3 and the more efficient Rayleigh scattering on the grains at shorter wavelengths [59, 99]. A spectral blue shift was also discovered in δ-phase GaQ_3 nanowires compared with β-phase GaQ_3 powder owing to a looser interligand spacing and reduced orbital overlap in their δ-phase molecular structures [58].

In a recent publication, the PL property of individual AlQ_3 nanorods was investigated by a Nd:YAG laser [74]. It could be seen that the maximum band of single AlQ_3 nanorods emission blue-shifted from 512 to 485 nm when compared to the PL spectrum of aggregated nanorods and a broad peak ranging from 520 to 620 nm emerged. This result was expected to enable scientists to explore novel applications in the field of optical devices.

At last, it is worth noting that the deliberate introduction of at least one kind of guest compound into the host material matrices, to some degrees, can induce novel luminescent properties. According to the molecular design, for one thing, Shinkai et al. [76, 77] and Gong et al. [78] introduced guest compounds to modify the molecules of MQ_n complexes and further synthesized the corresponding gel nanofibers with novel luminescence. For another, the introduction of metal, inorganic, and organic materials into the host of 1D MQ_n complex nanomaterials explored new luminescent properties and applications. Take Zhu and co-workers' report [72] for an example, the combination of the luminescent CdQCl complex nanowires and the biocatalytic growth of Au nanoparticles could be used to develop novel fluorescent sensing, which the fluorescence of the CdQCl complex nanowires was quenched by increasing the Au nanoparticle concentration.

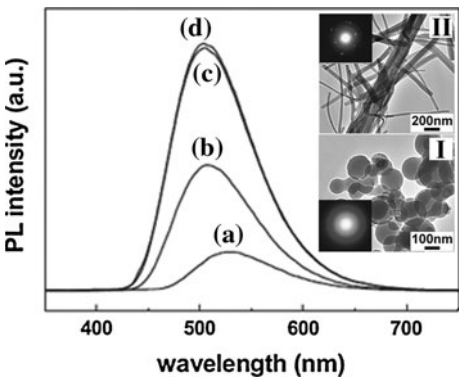

Fig. 7 PL spectra of AlQ_3: (*a*) amorphous nanoparticles; and nanopaticles heated in 1.33×10^4 Pa of Ar at 150 °C for (*b*) 1 min, (*c*) 6 min, and (*d*) 10 min. The *inset* TEM images and electron diffraction patterns show (I) the amorphous nanoparticles and (II) the crystalline nanowires corresponding to (*a*) and (*d*), respectively [55, 56]

Field emission

Since AlQ_3 nanowires first synthesized for field emission [45], 1D nanostructured MQ_n complexes and their derivatives have been continuously investigated because of their unique field emission properties and potential applications in field emission flat panel displays (FEDs).

For example, the hexagonal AlQ_3 nanorods showed a good field emission performance reported by Lee and co-workers [41]. Figure 8 presents the field emission characteristics by a typical curve of current density J versus applied electrical field E. The AlQ_3 nanorods exhibited a very low turn-on field of about 3.1 V μm^{-1} and a maximum current density of about 1.38 mA cm^{-2} at an applied field of 5.7 V μm^{-1}. The turn-on field was comparable to that of organic charge-transfer complex nanowires [100], but lower than that of some inorganic nanomaterials [101, 102]. The field emission characteristic was further analyzed with the Fowler–Nordheim (FN) theory described by $\ln(J/E^2) = \ln(A\beta^2/\Phi) + (-B\Phi^{3/2}/\beta)\ (1/E)$, where A and B were constants ($A = 1.54 \times 10^{-6}$ A eV V^{-2} and $B = 6.83 \times 10^9$ Vm^{-1} $eV^{-3/2}$), Φ is work function of the emitting materials, and β is field enhancement factor related to the emitter geometry [45]. The plot of $\ln(J/E^2)$ versus $(1/E)$ showed a straight line with a slope of about -27 at high applied field (inset of Fig. 8), demonstrating the field emission phenomenon [103]. Assuming a work function of $\Phi = 3.0$ eV for AlQ_3 [45], the β value was estimated to be about 1300 based on the above FN equation, which could be ascribed to the higher carrier mobility

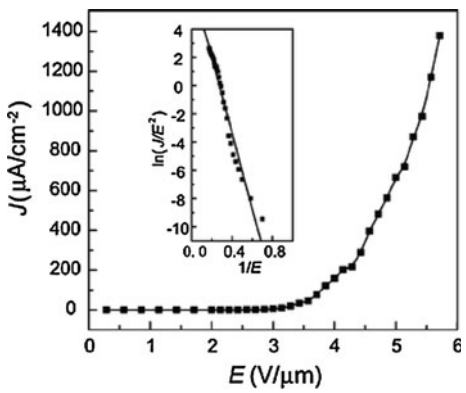

Fig. 8 Field emission J–E curve of the AlQ_3 nanorods and the corresponding FN plot (*inset*) [41]

or conductivity expected in the crystalline AlQ_3 nanorods. In contrast, AlQ_3 nanowires also exhibited a good field emission property with a relative low turn-on field of 3.7 V μm^{-1}, but a very high maximum current density above 16 mA cm^{-2} [38].

Compared with AlQ_3 nanowires and other film emitters, the AlQ_3 nanoprotrusions exhibiting a relatively lower emission threshold field were recently reported [104]. The electrons were emitted from an effective area on the tip of the nanoprotrusions. Both larger thickness and smaller effective protrusion radius could lead to enhanced field emission. A linear relationship between the effective and measured radii of the AlQ_3 nanoprotrusions demonstrated that surface roughness indeed had a significant influence on the field emission efficiency.

Besides, the field emission performances of the gel nanofibers assembled from 8-hydroxyquinolinol/copper(II)-, palladium(II)-, and platinum(II)-chelate based organogelators were also discussed [77]. Very interestingly, the field emission characteristics of these gel nanofibers were evidently different depending on the central metals although their shapes were almost the same. That result implied that the field emission performances of organometallic nanofibers with the same shape could be easily controlled by changing the central metals in the metallogel system. This opens a new way, especially in the nanoscale region, to control the turn-on field value by molecular design and modification.

Charge transport

As is well known, AlQ_3 is a typical electron-transport dominant material of MQ_n complexes and widely employed in OLEDs. Following this point, some efforts devoted to 1D nanostructures of this material have focused on their charge transport properties for optoelectronic device [42, 91].

As an example, Bi et al. [91] fabricated the single-carrier devices based on the films composed of *fac*-AlQ_3 (*fac* = facial) or *mer*-AlQ_3 (*mer* = meridional) nano/microrods, and they demonstrated that the configuration of AlQ_3 molecules had a dramatic effect on the transporting properties of AlQ_3 nanorods. The hole-only devices with structure of [ITO/active layer/Au] (active layer = *fac*-AlQ_3 nano/microrods-based film, or *mer*-AlQ_3 nano/microrods-based film, or amorphous AlQ_3 film) were studied. As expected, the *mer*-AlQ_3 nano/microrods-based film and amorphous AlQ_3 film exhibited very poor hole-transporting abilities. In contrast, the *fac*-AlQ_3 nano/microrods-based film displayed a remarkable hole-transporting feature. That characteristic of the hole-only device indicated that *fac*-AlQ_3 was a typical p-type semiconductor with good hole-transporting ability, which was totally different from *mer*-AlQ_3 with electron-transporting nature as an n-type semiconductor. Considering their excellent charge transport properties and controllable structures, the AlQ_3 nanorods might be find utilization in optoelectronics, such as OLEDs and organic filed-effect transistors (OFETs).

Photoconductivity and photo-switching

In addition to the interesting luminescence, filed emission, and charge transport properties discussed in previous three sections, recent work by Shao's group [42, 43, 65, 105] suggested that a series of 1D MQ_n complex nanomaterials could be found potential applications in nanoscale optoelectronic devices, owing to their unique photoconductive and photo-switching characteristics.

Among, the strong and stable luminescent ZnQ_2 nanoribbons were found to be sensitive to light [43]. As shown in Fig. 9a, the *I–V* curves measured in dark (curve I) and under illumination (curve II) both exhibited good linear behavior, which proved a fine ohmic contact between the ZnQ_2 nanoribbons and Au electrodes. The current of the nanoribbons rapidly increased under illumination with an incandescence lamp. In these cases, the energy from the light excited the electrons in the ZnQ_2 semiconductor nanoribbons from the valence band into the conduction band, increasing the charge carrier concentration via direct electron–hole pair creation and thus enhancing the current of the nanoribbons. Figure 9b shows the reversible photoresponse characteristic of the ZnQ_2 nanoribbons during light switching on/off. Obviously, the current through the ZnQ_2 promptly increased or decreased in accordance with the illumination on/off. It was suggested that the ZnQ_2 nanoribbons showed high photo-sensitivity, the current of which was enormously enhanced by approximately 24 times compared with the current in dark.

Likewise, the AlQ_3, CdQ_2, and MgQ_2 nanoribbons exhibited the excellent photoconductivity, and fast, reversible photo-switching responses under on/off light exposure conditions [42, 65, 105]. These MQ_n complex nanoribbons with unique optoelectronic properties are thought to be useful in the fabrication of photo-sensor and photo-switch nanodevices in the future.

Applications of 1D MQ_n complex nanomaterials

The most fundamental application of 1D MQ_n complex nanomaterials was to construct various optoelectronic devices, such as LED devices [50, 91], photo-sensors [39, 72], and photo-switches [42, 43, 105] based on wire-like, rod-like, or ribbon-like MQ_n complex nanomaterials. When they were fabricated into LED devices, take AlQ_3 nanowires, for instance, the performance of the resultant devices was enhanced considerably on decreasing the wire

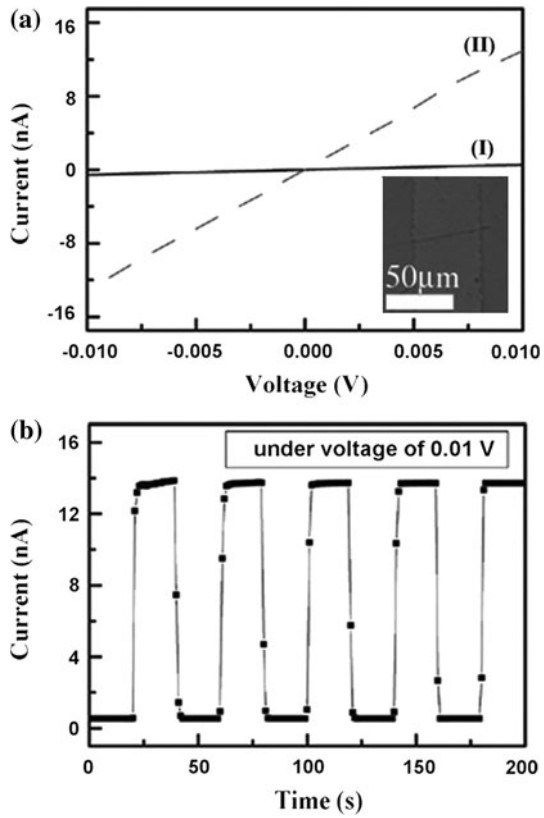

Fig. 9 **a** *I–V* curves of a bundle of ZnQ_2 nanoribbons measured in dark (curve I) and under illumination by using an incandescence lamp (12 V, 10 W) (curve II), and the optical microscope image of a bundle of ZnQ_2 nanoribbons between two Au electrodes (*inset*). **b** Photoresponse characteristics of the device during light switching on/off. A voltage of 0.01 V was applied across the Au–Au electrodes, and the current was recorded during the light alternatively on and off at 20 s intervals [43]

diameter [50]. Using the driving voltage of 12.5 V, the external quantum efficiencies of the devices prepared from AlQ_3 nanowires with diameters of 80, 60, and 40 nm were 0.28, 0.58, and 0.90%, respectively. When these materials applied in sensing, the ZnQ_2 nanorods were found to be sensitive to several proteins, such as human serum albumin (HSA), bovine serum albumin (BSA), bovine hemoglobin (Hb), and egg albumin (EA), displaying protein-concentration dependence of both PL and resonance light scattering (RLS), which provided a feasible way to build photo-sensors and probes [39]. Contrastively, the CdQCl nanowires, when combined with biocatalytic growth of Au nanoparticles, could be developed into a new fluorescence sensor for H_2O_2 and glucose detection [72].

Another important utilization of these materials was display application owing to their unique field emission characteristics [38, 41, 45]. Most of 1D MQ_n complex nanomaterials and their derivatives exhibited the stable field emission behavior, relatively low-threshold voltage and high-emission current density, implying these materials were attractive emitters for field emission application [48–50, 73]. Numerous advantages of these materials, such as low-cost, easy preparation, and good flexibility would be favored in the fabrication of field emission displays.

In addition, these 1D organometallic nanostructures were considered to be novel wire-templates for the preparation of different nanomaterials. Such as GaQ_3 nanowires were used as wire-templates to form alumina nanotubes after the removal of GaQ_3 templates by dissolving in toluene or by heat treatment [49].

Conclusions and outlook

MQ_n complexes belong to one class of the most important light-emitting and electron-transporting materials. Their 1D nanomaterials are good candidates for the development of micro/nano-scale devices, sensors, and other novel applications due to their flexible structures, excellent optoelectronic properties, and various synthetic strategies. This article reviews current progress in the synthesis of 1D nanostructrured MQ_n complexes and summarizes their optoelectronic properties and applications. Although diverse synthesis strategies including vapor phase growth, solution phase growth, self-assembly, and several new methods have been developed, precise control of their structures and performances, as well as systematic investigation of the habits of MQ_n nucleation and growth are relatively lacking. Much effort has so far been made to promote their applications associated with the intriguing properties including luminescence, field emission, charge transport, photoconductivity, and photo-switching. However, the depicted application researches, such as LED devices, photo-sensors, photo-switches, filed emission, and templates, are still limited in laboratory.

Therefore, many challenges remain in this area. First, there are strong requirements to develop universal and facile methods for the synthesis of 1D nanoscale MQ_n complexes with desired morphology and size, especially for the fabrication of hollow nanotubes, three-dimensional (3D) hierarchitectures and advanced composites. Second, another challenge is to promote the applications of the devices based on them to an industrial level. The overall performances of their devices need to be improved, and new application areas including solar cells and organic transistors should be exploited. Thirdly, in order to obtain 1D MQ_n nanomaterials with unique properties and controllable structures, the molecular design and modification of MQ_n complexes are still a great challenge as well as a good chance. The above aspects of 1D nanostructured MQ_n complexes and derivatives, though still in their infancies, provide many prosperous opportunities for researchers in the area of organometallic nanomaterials.

Acknowledgement This work was financially supported by the National Science Foundation of Fujian Province of China (No. 2009J01240). The authors express great thanks to Yani (Nicole) Wang, Xi'an International Studies University, for her critical reading and kind advices of this article.

References

1. Tang CW, VanSlyke SA (1987) Appl Phys Lett 51:913
2. Higginson KA, Zhang XM, Papadimitrakopoulos F (1998) Chem Mater 10:1017
3. Liao SH, Shiu JR, Liu SW, Yeh SJ, Chen YH, Chen CT, Chow TJ, Wu CI (2009) J Am Chem Soc 131:763
4. Kaji H, Kusaka Y, Onoyama G, Horii F (2006) J Am Chem Soc 128:4292
5. Burrows PE, Sapochak LS, McCarty DM, Forrest SR, Thompson ME (1994) Appl Phys Lett 64:2718
6. Sapochak LS, Benincasa FE, Schofield RS, Baker JL, Riccio KKC, Fogarty D, Kohlmann H, Ferris KF, Burrows PE (2002) J Am Chem Soc 124:6119
7. Chen W, Peng Q, Li YD (2008) Cryst Growth Des 8:564
8. Ouyang JM, Zhang ZM, Ling WH, Liu HY, Lu ZH (1999) Appl Surf Sci 151:67
9. Hamada Y, Sano T, Fujita M, Fujii T, Nishio Y, Shibata K (1993) Jpn J Appl Phys 32:L514
10. Khaorapapong N, Kuroda K, Ogawa M (2002) Clays Clay Miner 50:428
11. Khaorapapong N, Ogawa M (2007) Appl Clay Sci 35:31
12. Khaorapapong N, Ogawa M (2008) J Phys Chem Solids 69:941
13. Khaorapapong N, Ogawa M (2010) J Phys Chem Solids 71:1644
14. Sapelli E, Brandão TAS, Fiedler HD, Nome F (2007) J Colloid Interface Sci 314:214
15. Shi YL, Fu YQ, Lü CL, Hui L, Su ZM (2010) Dyes Pigments 85:66
16. Shen Y, Peng J, Chen CY, Zhang HQ, Meng CL, Li XL (2010) Inorg Chem Commun. doi:10.1016/j.inoche.2010.10.027
17. Cho CP, Perng TP (2006) Nanotechnology 17:3756
18. Guo Y, Wang ZB, Cui YP, Zhang JY, Ye YH (2008) Chin Phys Lett 25:4428
19. Mahmoud ME, Haggag SS, Abdel-Fattah TM (2009) Polyhedron 28:181
20. Mahmoud ME, Haggag SS, Rafea MA, Abdel-Fattah TM (2009) Polyhedron 28:3407
21. Li HB, Li YL (2009) Nanoscale 1:128
22. Barth S, Hernandez-Ramirez F, Holmes JD, Romano-Rodriguez A (2010) Prog Mater Sci 55:563
23. Lou XW, Archer LA, Yang ZC (2008) Adv Mater 20:3987
24. Zhao YS, Fu HB, Peng AD, Ma Y, Xiao DB, Yao JN (2008) Adv Mater 20:2859
25. Ng AMC, Djurišić AB, Tam KH, Kwok WM, Chan WK, Tam WY, Phillips DL, Cheah KW (2008) Adv Funct Mater 18:566
26. Goldstein AN, Echer CM, Alivisatos AP (1992) Science 256:1425
27. Yuan JJ, Zhou SX, Gu GX, Wu LM (2005) J Mater Sci 40:3927. doi:10.1007/s10853-005-0714-8
28. Li ZB, Deng YD, Wu YT, Shen B, Hu WB (2007) J Mater Sci 42:9234. doi:10.1007/s10853-007-1897-y
29. Ball P, Garwin L (1992) Nature 355:761
30. Wang C, Wang XM, Zhao JC, Mai BX, Sheng GY, Peng PA, Fu JM (2002) J Mater Sci 37:2989. doi:10.1023/A:1016077216172
31. Reed MA, Frensley WR, Matyi RJ, Randall JN, Seabaugh AC (1989) Appl Phys Lett 54:1034
32. Barbara B, Chudnovsky EM (1990) Phys Lett A 145:205
33. Takagahara T (1993) Phys Rev B 47:4569
34. Chen W, Ahmed H, Nakazoto K (1995) Appl Phys Lett 66:3383
35. Law M, Goldberger J, Yang PD (2004) Annu Rev Mater Res 34:83
36. Cheung CH, Djurišić AB, Leung YH, Wei ZF, Xu SJ, Chan WK (2004) Chem Phys Lett 394:203
37. Hrudey PCP, Szeto B, Brett MJ (2006) Appl Phys Lett 88:251106
38. Xu G, Tang YB, Tsang CH, Zapien JA, Lee CS, Wong NB (2010) J Mater Chem 20:3006
39. Pan HC, Liang FP, Mao CJ, Zhu JJ, Chen HY (2007) J Phys Chem B 111:5767
40. Lee T, Chang SC, Peng JF (2010) Thin Solid Films 518:5488
41. Hu JS, Ji HX, Cao AM, Huang ZX, Zhang Y, Wan LJ, Xia AD, Yu DP, Meng XM, Lee ST (2007) Chem Commun 29:3083
42. Wang XH, Shao MW, Shao G, Wang SW (2009) J Nanosci Nanotechnol 9:4709
43. Wang XH, Shao MW, Liu L (2010) Synth Met 160:718
44. Zhu J, Qian XF (2010) Solid State Sci 12:1314
45. Chiu JJ, Kei CC, Perng TP, Wang WS (2003) Adv Mater 15:1361
46. Chiu JJ, Wang WS, Kei CC, Perng TP (2003) Appl Phys Lett 83:347
47. Chiu JJ, Wang WS, Kei CC, Cho CP, Perng TP, Wei PK, Chiu SY (2003) Appl Phys Lett 83:4607
48. Cho CP, Perng TP (2010) Org Electron 11:115
49. Wang CC, Kei CC, Yu YW, Perng TP (2007) Nano Lett 7:1566
50. Zhao YS, Di CA, Yang WS, Yu G, Liu YQ, Yao JN (2006) Adv Funct Mater 16:1985
51. Tian XK, Fei JB, Pi ZB, Yang C, Luo DY, Pei F, Zhang LD (2006) Solid State Commun 138:530
52. Burke F, Abid M, Stamenov P, Coey JMD (2010) J Magn Magn Mater 322:1255
53. Hrudey PCP, Westra KL, Brett MJ (2006) Adv Mater 18:224
54. Zhang J, Salzmann I, Schäfer P, Oehzelt M, Duhm S, Rabe JP, Koch N (2009) J Mater Res 24:1492
55. Cho CP, Yu CY, Perng TP (2006) Nanotechnology 17:5506
56. Cho CP, Wu CA, Perng TP (2006) Adv Funct Mater 16:819
57. Morales AM, Lieber CM (1998) Science 279:208
58. Yu YW, Cho CP, Perng TP (2009) Nanoscale Res Lett 4:820
59. Brinkmann M, Gadret G, Muccini M, Taliani C, Masciocchi N, Sironi A (2000) J Am Chem Soc 122:5147
60. Dai ZR, Pan ZW, Wang ZL (2003) Adv Funct Mater 13:9
61. Trentler TJ, Hickman KM, Goel SC, Viano AM, Gibbons PC, Buhro WE (1995) Science 270:1791
62. Trentler TJ, Goel SC, Hickman KM, Viano AM, Chiang MY, Beatty AM, Gibbons PC, Buhro WE (1997) J Am Chem Soc 119:2172
63. Ma DK, Zhang JH, Hu XK, Zhou HY, Qian YT (2007) Chem Lett 36:630
64. Firsching FH, Brewer JG (1963) Anal Chem 35:1630
65. Wang XH, Shao MW, Liu L (2010) J Mater Sci: Mater Electron. doi:10.1007/s10854-010-0098-7
66. Patzke GR, Krumeich F, Nesper R (2002) Angew Chem Int Ed 41:2446
67. Xia YN, Yang PD, Sun YG, Wu YY, Mayers B, Gates B, Yin YD, Kim F, Yan HQ (2003) Adv Mater 15:353
68. Lin H, Wang BX, Wei ZJ (2008) Chin J Process Eng 8:157 (in Chinese)
69. Yin ZG, Wang BX, Chen GH (2010) Acta Chim Sin 68:1765
70. Wang BX, Lin H, Yin ZG (2011) Mater Lett 65:41
71. Mao CJ, Wang DC, Pan HC, Zhu JJ (2010) Ultrason Sonochem 18:473
72. Pan HC, Lin HY, Shen QM, Zhu JJ (2008) Adv Funct Mater 18:3692
73. Uthirakumar P, Suh EK, Hong CH (2008) J Lumin 128:1629
74. Chen W, Peng Q, Li YD (2008) Adv Mater 20:2747

75. Gao JX, Bender CM, Murphy CJ (2003) Langmuir 19:9065
76. Shirakawa M, Fujita N, Tani T, Kaneko K, Shinkai S (2005) Chem Commun 33:4149
77. Shirakawa M, Fujita N, Tani T, Kaneko K, Ojima M, Fujii A, Ozaki M, Shinkai S (2007) Chem Eur J 13:4155
78. Kong S, Xiao LX, Chen ZJ, Yan XZ, Qu B, Wang SF, Gong QH (2010) New J Chem 34:325
79. Terech P, Weiss RG (1997) Chem Rev 97:3133
80. Hashimoto M, Ujiie S, Mori A (2003) Adv Mater 15:797
81. Barberá J, Cavero E, Lehmann M, Serrano JL, Sierra T, Vázquez JT (2003) J Am Chem Soc 125:4527
82. Yoshio M, Mukai T, Ohno H, Kato T (2004) J Am Chem Soc 126:994
83. Li XQ, Stepanenko V, Chen ZJ, Prins P, Siebbeles LDA, Würthner F (2006) Chem Commun 37:3871
84. Rueping M, Antonchick AP, Theissmann T (2006) Angew Chem Int Ed 45:3683
85. Li XZ, Yu R, Wei XW (2010) Chem Lett 39:114
86. Shin HW, Shin EJ, Cho SY, Oh SL, Kim YR (2007) J Phys Chem C 111:15391
87. Yang PP, Chen JF, Huang ZH, Zhan SM, Jiang ZJ, Qiu YQ, Shao C (2009) Mater Lett 63:1978
88. Yan E, Wang C, Huang ZH, Xin Y, Tong YB (2007) Mater Sci Eng A 464:59
89. Yan E, Huang ZH, Xin Y, Zhao Q, Zhang W (2006) Mater Lett 60:2969
90. Liu L, Wang L, Jia DZ (2008) J Coord Chem 61:1019
91. Bi H, Zhang HY, Zhang Y, Gao HZ, Su ZM, Wang Y (2010) Adv Mater 22:1631
92. Hulteen JC, Martin CR (1997) J Mater Chem 7:1075
93. Song YJ, Garcia RM, Dorin RM, Wang HR, Qiu Y, Coker EN, Steen WA, Miller JE, Shelnutt JA (2007) Nano Lett 7:3650
94. Wan MX (2008) Conducting polymers with micro or nanometer structure. Springer, Berlin
95. Li D, Xia YN (2004) Adv Mater 16:1151
96. Li D, Wang YL, Xia YN (2003) Nano Lett 3:1167
97. Sigmund W, Yuh J, Park H, Maneeratana V, Pyrgiotakis G, Daga A, Taylor J, Nino JC (2006) J Am Ceram Soc 89:395
98. Alivisatos AP (1996) Science 271:933
99. Djurišić AB, Lau TW, Lam LSM, Chan WK (2004) Appl Phys A 78:375
100. Liu HB, Zhao Q, Li YL, Liu Y, Lu FS, Zhuang JP, Wang S, Jiang L, Zhu DB, Yu DP, Chi LF (2005) J Am Chem Soc 127:1120
101. Lee CJ, Lee TJ, Lyu SC, Zhang Y, Ruh H, Lee HJ (2002) Appl Phys Lett 81:3648
102. Li YB, Bando Y, Golberg D, Kurashima K (2002) Appl Phys Lett 81:5048
103. Heer WA, Châtelain A, Ugarte D (1995) Science 270:1179
104. Cho CP, Perng TP (2007) Nanotechnology 18:12502
105. Wang XH, Shao MW, Liu L (2010) Thin Solid Films 519:231